AGU PUBLICATIONS

Global Biogeochemical Cycles

RESEARCH ARTICLE
10.1002/2014GB004822

Key Points:
- Grassland expansion affected oxygen isotopes of precipitation composition
- Isotope records record plant ecosystem changes
- Recycling of water vapor must be taken into account in paleoclimate studies

Supporting Information:
- Text S1
- Figure S1a
- Figure S1b
- Figure S1c
- Figure S1d
- Figure S1e
- Table S1

Correspondence to:
C. P. Chamberlain,
chamb@stanford.edu

Citation:
Chamberlain, C. P., M. J. Winnick, H. T. Mix, S. D. Chamberlain, and K. Maher (2014), The impact of neogene grassland expansion and aridification on the isotopic composition of continental precipitation, *Global Biogeochem. Cycles*, *28*, doi:10.1002/2014GB004822.

Received 4 FEB 2014
Accepted 23 AUG 2014
Accepted article online 27 AUG 2014

The impact of neogene grassland expansion and aridification on the isotopic composition of continental precipitation

C. P. Chamberlain[1], M. J. Winnick[1], H. T. Mix[1], S. D. Chamberlain[2], and K. Maher[3]

[1]Department of Environmental Earth Systems Science, Stanford University, Stanford, California, USA, [2]Department of Ecology and Evolutionary Biology, Cornell University, Ithaca, New York, USA, [3]Department of Geological and Environmental Sciences, Stanford University, Stanford, California, USA

Abstract The late Cenozoic was a time of global cooling, increased aridity, and expansion of grasslands. In the last two decades numerous records of oxygen isotopes have been collected to assess plant ecological changes, understand terrestrial paleoclimate, and to determine the surface history of mountain belts. The $\delta^{18}O$ values of these records, in general, increase from the mid-Miocene to the Recent. We suggest that these records record an increase in aridity and expansion of grasslands in midlatitude continental regions. We use a nondimensional isotopic vapor transport model coupled with a soil water isotope model to evaluate the role of vapor recycling and transpiration by different plant functional types. This analysis shows that increased vapor recycling associated with grassland expansion along with biomechanistic changes in transpiration by grasses themselves conspires to lower the horizontal gradient in the $\delta^{18}O$ of atmospheric vapor as an air mass moves into continental interiors. The resulting signal at a given inland site is an increase in $\delta^{18}O$ of precipitation with the expansion of grasslands and increasing aridity, matching the general observed trend in terrestrial Cenozoic $\delta^{18}O$ records. There are limits to the isotopic effect that are induced by vapor recycling, which we refer to here as a "hydrostat." In the modern climate, this hydrostatic limit occurs at approximately the boundary between forest and grassland ecosystems.

1. Introduction

One of the most profound ecological changes during the Cenozoic was the expansion of grasslands in the Middle to Late Miocene [*Cerling et al.,* 1993]. This expansion occurred during a time of global cooling [*Zachos et al.,* 2001] and increased aridification [*Osborne*, 2008]. As grasslands replaced forests and shrubs they influenced mammalian evolution [*Janis*, 1993] and altered the silica [*Kidder and Gierlowski-Kordesch*, 2005] and carbon cycles [*Retallack*, 2001]. The expansion of grasslands may have affected the hydrologic cycle as well. Herein, we examine Neogene global oxygen isotope records using a one-dimensional isotopic vapor transport and coupled soil isotope model. We argue that the rise of grasslands and increased aridification in the Miocene affected the water balance of midlatitude regions. Consequently, the general trend of increasing $\delta^{18}O$ of authigenic minerals in paleosols and in fossils observed worldwide (Figure 1) could be caused by increased evaporative and transpirative fluxes relative to runoff during a time when grasslands replaced forest ecosystems in the Middle Miocene.

Modulation of the hydrologic cycle by plants is apparent in both modern and ancient systems [*Berry et al.,* 2010]. At present, evapotranspirative (ET) fluxes account for over half of the total continental precipitation worldwide [*Oki and Kanae*, 2006]. Modern changes to this ET flux induced by altering plant communities through large-scale deforestation have been shown to change precipitation patterns at both the local scale and mesoscale [*Garcia-Carreras and Parker*, 2011; *Lee et al.,* 2012]. Globally, precipitation patterns are strongly affected by vapor recycling by plants, particularly in the midlatitudes [*Kleidon et al.,* 2000]. Ancient hydrologic cycles have also been altered by shifts in plant community. For example, expansion of angiosperms in the Cretaceous had profound effects on the global hydrologic cycle because flowering plants transpired more water than preexisting vegetation [*Boyce and Lee*, 2010]. We argue that similar changes in the hydrologic cycle must have occurred in the Miocene as grasslands, with different transpirational properties, replaced forest ecosystems.

Trees and grasses differ in several ways in their ability to transpire water, and thus, the hydrological balance in these two ecosystems is fundamentally different. First, grasses have the ability to affect the hydrologic cycle

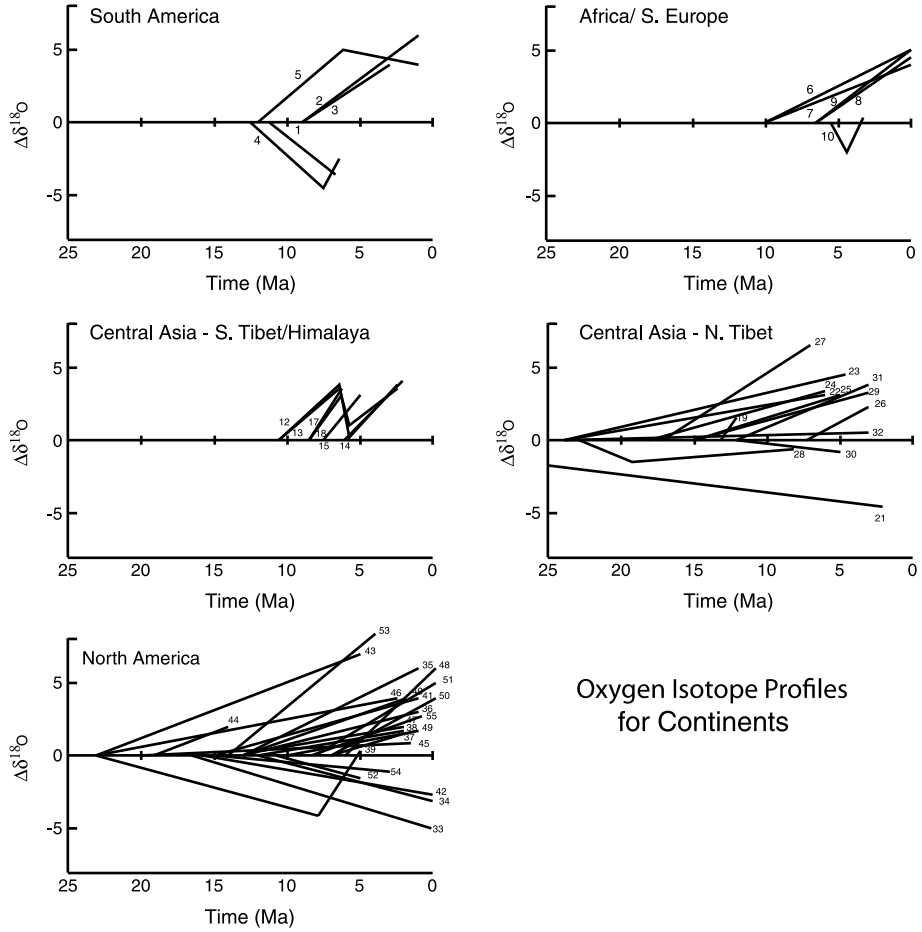

Figure 1. Summary diagrams showing the amount and timing of the oxygen isotope changes in the terrestrial sections. These simplified isotope trends show only how much change has occurred in the isotope record ($\Delta\delta^{18}O$) and the timing. The numbers on the lines are keyed to the studies given in Table S1 in the supporting information.

through their unique stomata. The stomata in grasses are "dumb bell" shaped as opposed to "kidney shaped" in other angiosperms. This evolutionary adaptation allows for rapid opening and closing of the stomata in response to periodic drought. Thus, grasses transpire water in much more punctuated periods compared to other angiosperms that lack the ability to rapidly open and close their stomata [*Hetherington and Woodward*, 2003]. Grasses transpire during wet periods and go to seed during dry periods. Therefore, their annual transpirational cycle is more seasonal than that of forests [*Ferretti et al.,* 2003]. Second, grasses have shallower root systems as compared to trees that tap deeper water sources. As a result, grasses have a greater ability to reduce soil water content than trees, which leads to a greater temporal variability in soil moisture content in grasslands [*James et al.,* 2003]. Finally, in grassland ecosystems total ET approaches total runoff, whereas in forest ecosystems ET is generally less than runoff [*Alton et al.,* 2009].

Changes in the hydrologic balance of a region will be recorded in the $\delta^{18}O$ of precipitation. For example, increased recharge of moisture to the atmosphere through high ET and reduction of runoff through increased aridity both will tend to reduce horizontal gradients in the $\delta^{18}O$ of precipitation along a storm track [*Ingraham and Craig*, 1993]. These isotopic changes must be manifested in the continental oxygen isotope record as grasslands expanded to replace forests and the midlatitudes became more arid during the Neogene. As such, this paper is motivated by the observation that the majority of oxygen isotope records of Neogene terrestrial basins show increasing $\delta^{18}O$ values with decreasing age (Figures 1 and 2; see Figures S1a–S1e in the supporting information). There are numerous and varied explanations for the large majority of records that show increasing $\delta^{18}O$ values through time. Interpretations range from increased aridity and soil water evaporation [*Quade et al.,* 1994], intensification of the Asian and North American monsoons [*Ghosh et al.,* 2004; *Horton and Chamberlain*, 2006], to a

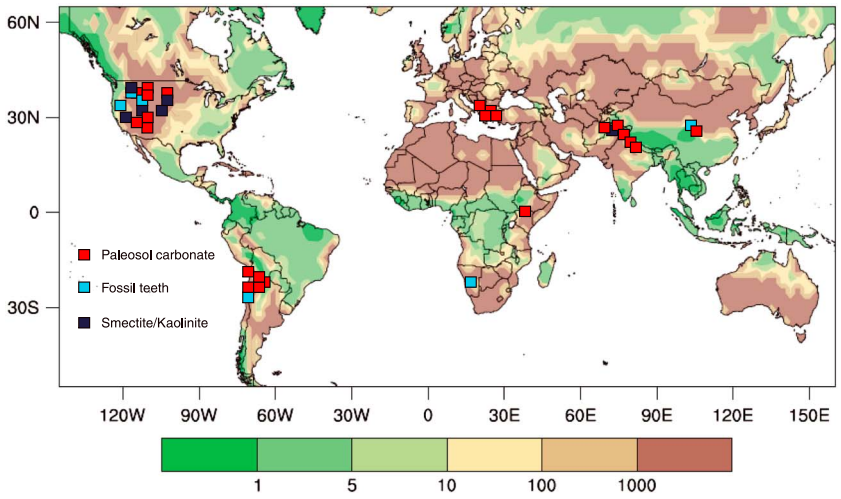

Figure 2. Global map of the Damköhler number (Nd_{ET}) for recycling of water vapor. Shown are the sample localities for the oxygen isotope profiles given in Figure 1 and Table S1 in the supporting information. We calculate Nd_{ET} using annual precipitation and latent heat fluxes from NCEP-DOE Reanalysis II from 1979 to 2012 [*Kanamitsu et al.,* 2002] and equation (10) in the main text. The map of Damköhler numbers is consistent with numerous site-specific studies of forests and grasslands that show ET/*Q* is greater for grasslands than forests [*Running and Coughlan*, 1988; *Dugas et al.,* 1996; *Kurc and Small*, 2004], thus confirming that, in general, Nd_{ET} of forests $<$ Nd_{ET} of grasslands.

change of atmospheric circulation patterns due to the uplift of Tibet [*Dettman et al.,* 2003] among others (see Table S1 in the supporting information). It is possible that each of these explanations is valid for their relevant study area and time frame. That said, we note that all of the isotopic records come from semiarid settings and from areas where grasslands have replaced forests and shrub lands (Figure 2). This observation begs the question: "What isotopic effects result from combined changes in plant functional types and aridity?" In a recent study of North American grasslands it has been suggested that the change of plant communities from forests to grasses induced an isotopic effect [*Mix et al.*, 2013]. Here we extend this research using a nondimensional form of an isotopic vapor transport model [*Hendricks et al.,* 2000] coupled to a soil water evaporation model [*Zimmermann et al.,* 1967] to evaluate global isotopic records. With this coupled model, we show that the effect of recycling of water vapor with the expansion of grasslands and increased aridity is manifest in nearly all of the long-term oxygen isotopic records across the globe.

2. Oxygen Isotope Global Data Set

We compiled published oxygen isotope data from terrestrial sections worldwide that are Neogene in age and represent long-term records (millions of years). These records come from pedogenic carbonate, lacustrine carbonate, pedogenic clays, and fossil biophosphate and calcite (Figures 1 and 2; see Figures S1a–S1e and Table S1 for full isotope records). The change in oxygen isotopic composition of the proxy ($\Delta\delta^{18}O$) shown in Figure 1 and given in Table S1 in the supporting information of this paper are those quoted from the relevant studies. For the majority of these records, the $\Delta\delta^{18}O$ increases with time. There are, however, a few notable exceptions. Sites on the leeward side of the Cascades of North America and a few in the Andes record a decrease in $\delta^{18}O$ values since the mid-Miocene (Figures S1a–S1e in the supporting information). These negative trends in $\delta^{18}O$ values in both regions are interpreted to be the result of increasing surface elevation of these two mountain ranges [*Takeuchi and Larson*, 2005; *Garzione et al.,* 2006].

For the following reasons, we dismiss the effects of global cooling and ice sheet growth as the primary reasons for the changes in isotopes observed in terrestrial records. First, while the growth of terrestrial ice sheets caused ocean water $\delta^{18}O$ to increase, this increase was relatively small (~0.8 to 1‰ during the Cenozoic[*Zachos et al.,* 2001]) as compared to the changes in $\delta^{18}O$ observed in terrestrial records (often greater than 3‰; Figures S1a–S1e and Table S1). Thus, the relatively modest change in ocean surface water

$\delta^{18}O$ is insufficient to drive the observed isotopic changes in water precipitated over land without further changes downstream of the ocean evaporation. Second, the global cooling that occurred since the Middle Miocene would result in a decrease in $\delta^{18}O$ of precipitation and paleosol carbonate rather than an increase for two reasons: (1) As global temperatures decrease the vertical isotopic gradient in the troposphere increases, leading to a decrease in $\delta^{18}O$ of precipitation, particularly over mountainous regions [*Poulsen and Jeffery*, 2011]. (2) The $\delta^{18}O$ of soil carbonate decreases in a colder environment because of the combined effects of temperature on the $\delta^{18}O$ of precipitation [*Rozanski et al.,* 1993] and the oxygen isotope fractionation between calcite and water [*Kim and O'Neil*, 1997].

3. Modeling

We use the isotopic vapor transport model developed by *Hendricks et al.* [2000] with transport by advection only. This formulation differs from the standard Rayleigh condensation models through the advection and ET terms. *Hendricks et al.* [2000] used this approach to examine the $\delta^{18}O$ and δD of precipitation for meridional vapor transport over the oceans and glaciated Antarctica. As such, her study required an eddy diffusion term for mixing between air masses along with evaporation of isotopically homogenous ocean water and sublimation of ice. Our formulation differs from theirs as: (1) we model vapor transport from a single air mass, and thus, eddy diffusion processes can be ignored; and (2) we must account for the isotopic composition of terrestrial evaporation and transpiration, which are dynamically related to the local isotopic composition of precipitation via environmental variables such as temperature and relative humidity. Thus, our calculations require a soil water model (see below) that couples to the isotopic vapor transport model. The coupling of these models occurs through the return water vapor (δ_{ET} in equation (4) below). Here grasslands in semiarid zones differ from forests by returning ^{18}O-enriched water from the upper 30 cm of soil (see below). We recognize that this is an oversimplification of soil water/atmospheric interactions due to soil physical properties, plant and soil water interactions, soil water storage, etc. However, these complexities are beyond the scope of our generalized model of atmospheric vapor transport and moisture recycling by plant ecosystems.

While originally used to model latitudinal-scale gradients over the ocean, the generalized mass balance equation (i.e., the mixing ratio) of water in the atmosphere is ubiquitous for the globe. Therefore, we argue that the use of the one-dimensional isotope vapor transport model captures the first-order isotopic mass balance between the atmosphere and land surface along continental air mass trajectories when transpiration and terrestrial evaporation fluxes are accounted for [*Winnick et al.*, 2014]. As a test, we have applied this model in dimensional form to central/western U.S. grasslands and it reproduces known continental isotopic gradients [*Mix et al.*, 2013]. However, because the model is not dynamic, it will not reproduce complicating effects such as convection [*Bony et al.,* 2008] and postcondensation isotopic fractionation [*Lee and Fung*, 2007]. For example, convection will result in a decrease in $\delta^{18}O$ values of precipitation ("the amount effect") and the trends discussed here could be reproduced if convection played a less dominate role during the Miocene to Recent aridification of the continents.

3.1. Isotopic Vapor Transport Model

The mass balance equation that relates the change of atmospheric water as a function of time is

$$\frac{dw}{dt} = \nabla(k\nabla w) - v\nabla w + \mathrm{ET} - P \tag{1}$$

where t time (s), w = concentration of total water in the atmosphere (m^3 water/m^2), K = eddy diffusion coefficient vector (m^2/t), v = wind velocity (m/s), ET = evapotranspiration rate (m^3 water/m^2 s), P = precipitation rate (m^3 water/m^2 s), and ∇ is the three-dimensional divergence operator.

The first term on the right-hand side of equation (1) represents mixing by eddy diffusion processes. The second term is the transport of water vapor by advection. The third and fourth terms represent sources and sinks of water by evapotranspiration and precipitation, respectively (for a discussion of the effects of eddy diffusive processes, see [*Winnick et al.*, 2014]). We simplify the model by assuming transport along a one-dimensional storm track by advection only. Thus,

$$\frac{dw}{dt} = -v\frac{dw}{dx} + \mathrm{ET} - P \tag{2}$$

We next write equation (2) for the two isotopologues of interest ($H_2{}^{18}O$ and $H_2{}^{16}O$; w_{18} and w_{16}) and use the chain rule to write the mass balance in terms of the ratio r_a of the isotopologues in the atmosphere (w_{18}/w_{16}):

$$\frac{dr_a}{dt} = -\frac{v}{w_{16}}\left(\frac{dw_{18}}{dx} - r_a\frac{dw_{16}}{dx}\right) + \frac{1}{w_{16}}(ET_{18} - r_aET_{16}) - \frac{1}{w_{16}}(P_{18} - r_aP_{16}) \quad (3)$$

We assume $w_{16} = w$, $ET_{16} = ET$, and $P_{16} = P$ based on the relative abundances of the isotopologues and rewrite equation (3) in δ notation assuming steady state

$$\frac{d\delta_a}{dt} = 0 = -v\frac{d\delta_a}{dx} + \frac{ET}{w}(\delta_{ET} - \delta_a) - \frac{P}{w}(\delta_P - \delta_a) \quad (4)$$

where δ_a, δ_{ET}, and δ_P are the $\delta^{18}O$ of atmospheric vapor, evapotranspiration, and precipitation, respectively. Next, we rewrite P in terms of ET and advection from equation (2) assuming steady state

$$0 = -v\left[\frac{d\delta_a}{dx} - \frac{1}{w}\frac{dw}{dx}(\delta_P - \delta_a)\right] + \frac{ET}{w}(\delta_{ET} - \delta_P) \quad (5)$$

In order to aid our discussion, equation (5) is written in terms of nondimensional parameters:

$$\frac{d\delta_a}{dx'} = (\delta_P - \delta_a) + Nd_{ET}(\delta_{ET} - \delta_P), \quad (6)$$

where

$$x' = \frac{x}{\ell}, \quad (7)$$

$$\ell = -w\frac{dx}{dw}, \quad (8)$$

and

$$Nd_{ET} = \frac{ET \cdot \ell}{vw} \quad (9)$$

In this formulation, x' is the dimensionless distance along a storm track, ℓ is the characteristic length scale of atmospheric moisture, and Nd_{ET} is a Damköhler number that relates the rate of ET to the rate of moisture transport. The benefit of using these parameters is that they allow us to examine the sensitivity of isotopic profiles along a storm track to environmental changes at any scale.

Finally, we use the analytical solution of equation (6) to solve for the $\delta^{18}O$ of atmospheric water vapor [*Hendricks*, 1999]:

$$\delta_a = \left(\delta_a^i - \delta_a^\infty\right)\exp[-x'(\alpha + Nd_{ET}\alpha - 1)] + \delta_a^\infty \quad (10)$$

where

$$\delta_a^\infty = \frac{Nd_{ET}\delta_{ET} - (1 + Nd_{ET})(\alpha - 1)10^3}{\alpha + \alpha Nd_{ET} - 1} \quad (11)$$

$\delta^i{}_a$ is the isotopic composition of initial vapor, and α is the equilibrium fractionation factor of condensation. We calculate local δ_P assuming equilibrium fractionation from δ_a. Note that when Nd_{ET} is zero, $\delta^\infty{}_a$ becomes -10^3 and equation (10) reduces to the traditional Rayleigh equation.

For a more intuitive understanding of the nature of Nd_{ET}, we can simplify its expression in equation (9) using the steady state form of equation (2) as

$$Nd_{ET} = \frac{ET}{P - ET} = \frac{ET}{Q} \quad (12)$$

where Q is runoff, assuming steady state conditions in soil moisture storage. In other words, Nd_{ET} is the ratio of moisture recycled back to atmosphere to moisture lost from the system via runoff.

Global annual Nd_{ET} calculated from National Centers for Environmental Prediction (NCEP)-Department of Energy (DOE) Reanalysis II latent heat flux and precipitation data from 1979 to 2012 [*Kanamitsu et al.*, 2002] is plotted in Figure 2. In general, Nd_{ET} is lowest (<1) on the windward side of mountain ranges when orographic precipitation far exceeds ET. Globally, Nd_{ET} increases as ET approaches P, either with lower precipitation rates or higher amounts of moisture recycling so that Nd_{ET} values above 10 are generally found in semiarid to

arid regions. In general, low Nd_{ET} values (<5) represent areas dominated by forest ecosystems while grasslands and deserts have higher Nd_{ET} values (>10) (Figure 2).

As mentioned above, there are a number of atmospheric processes that are not captured in the model that should differ between grassland and forest ecosystems. For example, changes in albedo, boundary layer, convective storms, etc. all would require a dynamic model that is beyond the scope of this paper. All of these processes should be expressed in the isotope values of precipitation to some degree. Moreover, we speculate that global aridification also contributed to a reduction in continental isotopic gradients through changes in postcondensational processes. Reductions in atmospheric relative humidity result in the enhanced evaporation of falling raindrops. Previous model studies have shown that this process results in higher $\delta^{18}O$ precipitation values through the evaporative enrichment of raindrops, along with the associated isotopic enrichment of ^{18}O in the subcloud moisture vapor via the increased reevaporated fraction of raindrops that acts to lower horizontal isotopic gradients [*Risi et al.,* 2008].

3.2. Isotope Soil Water Model

To incorporate the effects of evaporation and transpiration of soil water in the moisture budget, we use an advection and diffusion equation for isotopes in soil water. The soil water equation is necessary because the isotopic composition of the return vapor flux from plants will depend on rooting depth. Thus, it is necessary to resolve the depth profile of $\delta^{18}O$ in the soil water due to evaporation.

The model we use to describe the distribution of oxygen isotopes in soil water is from *Zimmermann et al.* [1967]. This model uses the following equations:

$$R_i = \left(R_{i,\mathrm{sur}} - R_{i,\mathrm{precip}}\right) \exp\left(\frac{-Z_i}{Z^*}\right) + R_{i,\mathrm{precip}} \tag{13}$$

where R_i is the $^{18}O/^{16}O$ of soil water, $R_{i,sur}$ is the $^{18}O/^{16}O$ of surface water, and $R_{i,precip}$ is the $^{18}O/^{16}O$ of input water or precipitation. Here z_i is the distance beneath the surface and z^* is the "decay length" given by

$$Z^* = \frac{D_i^*}{E_{\mathrm{soil}}} \tag{14}$$

In this equation E_{soil} is the evaporation rate (m^3 water/m^2 sec) from the soil surface. D_i^* is the effective diffusivity (m^2/s) of species i in soil water and is calculated using the relationship:

$$D_i^* = \rho \cdot \tau \cdot D_i \tag{15}$$

where ρ is the porosity of the soil, τ is the effective tortuosity, and D_i is the diffusion coefficient of species i in liquid water.

$R_{i,sur}$ of surface water of the soil profile is calculated using the relative humidity, and the isotopic ratios ($^{18}O/^{16}O$) precipitation ($R_{i,precip}$) and atmospheric vapor ($R_{i,vapor}$) determined for each distance step in equation (10). The isotopic value of surface water is given by

$$R_{i,\mathrm{sur}} = \alpha_{\mathrm{eq}} \cdot \left[(1-h) \cdot \alpha_{\mathrm{kin}} \cdot R_{i,\mathrm{precip}} + h \cdot R_{i,\mathrm{vapor}}\right] \tag{16}$$

Here α_{eq} and α_{kin} are the equilibrium and kinetic fractionation factors for water and vapor and h is the relative humidity.

The model of *Zimmermann et al.* [1967] assumes steady state evaporation and diffusion in a saturated soil. We realize that infiltration events and the presence of a vapor phase in unsaturated soils will complicate the isotope soil water profiles [*Allison*, 1982; *Barnes and Allison*, 1983; *DePaolo et al.,* 2004]. The presence of a vapor phase will cause the $\delta^{18}O$ of soil water to decrease in the upper few centimeters of the soil column from a maximum value that lies slightly below the soil surface. It is beyond the scope of this paper to capture this level of detail in our calculations, as our goal is to understand the broad effects of changing vegetation type and aridity on the $\delta^{18}O$ of precipitation and soil water.

The use of the *Zimmermann et al.* [1967] equations in our calculations is supported by observations of the $\delta^{18}O$ of soil water and carbonate from modern soils in semiarid regions. The $\delta^{18}O$ of both soil water and carbonate increase in the top ~30 cm of the soil often by as much as 5 to 8‰ (Figure 3). This increase is due to the upper wicking of water as the soil dries. These profiles are a function of soil properties (porosity and tortuosity), soil water

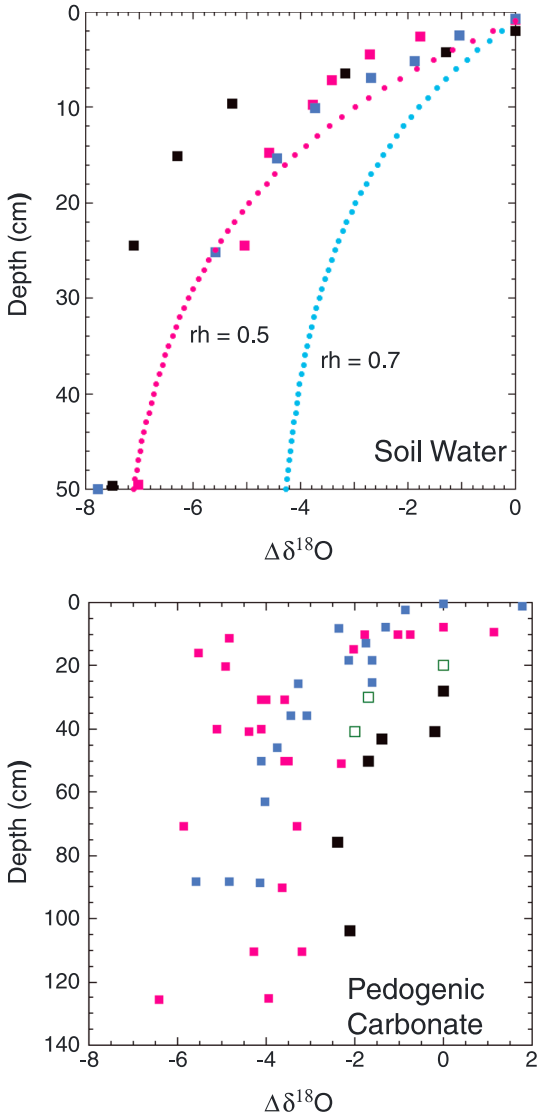

Figure 3. $\delta^{18}O$ of soil water in soils. For comparison, all $\delta^{18}O$ values are reported with respect to surface water $\delta^{18}O$ values ($\Delta\delta^{18}O$). Shown are three measured $\delta^{18}O$ profiles for soil waters collected from a Colorado grassland [*Ferretti et al.,* 2003]. The dotted lines represent calculated $\delta^{18}O$ soil water values for two different relative humidities. Also shown are the $\delta^{18}O$ of soil carbonate in soils. These values come from *Quade et al.* [1989b] (red and blue small squares) and *Liu et al.* [1996] (open black and solid large squares). For additional profiles see *Breecker et al.* [2012].

evaporation rates, and changes in relative humidity at the soil surface. The parameters used for this model are discussed below.

3.3. Parameters for Model

In all of the model runs presented here, we use the following values as constants. The $\delta^{18}O$ of evaporative water is a function of both equilibrium and kinetic processes, which we calculate using the equilibrium fractionation factor between water liquid and vapor [*Horita and Wesolowski*, 1994] and the expression of *Gonfiantini* [1986] for kinetic effects. For porosity (ρ) and tortuosity (τ), we selected values that were indicative of grassland soils. We use $\rho = 0.5$ that is typical of grassland in semiarid regions [*Evrendilek et al.,* 2004; *Wilson and Paz-Ferreiro*, 2012, and references therein]. The effective tortuosity (τ) varies from 0.7 in uniform sand to as low as 0.3 in clay. We use a median value of 0.5 for these calculations. We recognize that these soil properties can vary widely in nature. Again, our intent is to model the first-order isotopic changes that are caused by aridity and changes in vegetation type. Changes in these values of 10% cause a change in the $\delta^{18}O$ composition of soil water at 30 cm depth (Figure 3) of only 0.5‰. One should note, however, that changing the tortuosity from sand (0.7) to clay (0.3) will have a strong effect on the isotope profiles in soils, by as much as 2.0‰ at 30 cm depth. Thus, the isotopic composition of transpired water will also depend upon soil type.

For all of these calculations, we use the values given in *Alton et al.* [2009] to calculate evaporation (E) and transpiration (T) fluxes for different plant functional types. The isotopic results that use these calculated ET values [*Alton et al.,* 2009] do not differ appreciably from results using site-specific measured ET values [see *Mix et al.*, 2013]. As mentioned in the text, we use representative rooting depths of grasses to be 0 to 30 cm and trees and shrubs at 1 m and greater [*Jackson et al.,* 1996], which is consistent with other studies that show that grasses tap the upper portions of soils relative to trees and shrubs [*Dugas et al.,* 1996; *Kurc and Small*, 2004]. Since the evaporative enrichment and wicking effect causes an increase in $\delta^{18}O$ of soil water in the upper 30 cm of soil the transpired vapor in grasslands will be greater than $\delta^{18}O$ of incoming precipitation. In contrast, the $\delta^{18}O$ of transpired water in forests will equal that of precipitation as at depths greater than 1 m the soil water $\delta^{18}O$ is the same as the $\delta^{18}O$ of precipitation for all values of relative humidity and evaporation rate (Figure 3). Thus, the role of soil water evaporation will be negligible in forests, which is consistent with the observation that the contribution to atmospheric water vapor by soil water evaporation in deciduous forest at midlatitudes is relatively low [*Wilson et al.,* 2001]. We note that this model does not capture the fact that trees can tap groundwater or sources of water that are seasonally isotopically distinct from that of soil water [*Ehleringer and Dawson*, 1992].

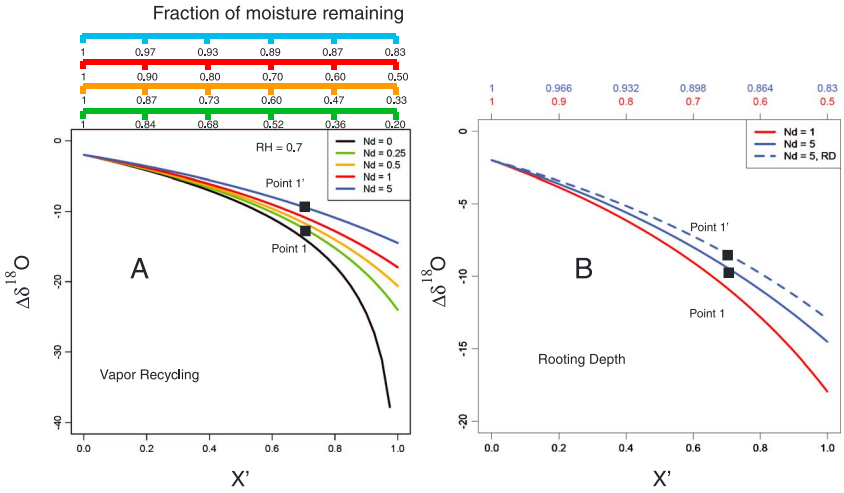

Figure 4. (a) Changes in the oxygen isotope composition of precipitation as a function of vapor recycling (Nd_{ET}) with no rooting depth effect. The colored axes at the top of the figure are the equivalent amount of fraction of moisture remaining in the atmosphere for different degrees of vapor recycling (Nd_{ET}) as compared to the situation where no vapor is recycled (black curve). The numbers are different Damköhler numbers. In these calculations $E = T$ and relative humidity is 0.7. Points 1 and 1′ are an idealized area on the land surface that has transitioned from a forest (1) to a grassland (1′). (b) Oxygen isotope changes in precipitation as a result of rooting depth for different amounts of vapor recycling. ($Nd_{ET} = 1$ and 5). Blue dashed curve shows the effects of shallow rooting grasses. All calculations are for a relative humidity of 0.7.

It is also important to note that in the following discussion, we analyze isotopic profiles across a dimensionless storm track, where distance varies from $x' = 0$ to 1 (equation (7)). This corresponds to the complete rainout of atmospheric moisture or cloud fraction ranging from 1 to 0 assuming no moisture recycling. This formulation assumes constant precipitation rates along the dimensionless profile, which is not necessarily representative of real-world storm tracks. Instead, the idealized scenarios presented here may be scaled to actual storm tracks with spatially varying rates of P and ET using the characteristic length scale (equation (8)), which is controlled by the atmospheric moisture gradient.

4. Results and Discussion

We investigated the response of the isotopic composition of precipitation as a result of changing conditions of water balance, plant rooting depth, and aridity as grasslands replace forest and shrub lands. We selected model parameters that are representative of these different ecosystems (see above).

We argue that the global increase in isotopes of precipitation as recorded in the isotope records (Figure 1) is a response to the increased aridity and expansion of grasslands in the Miocene. We recognize that global cooling along with changes in ocean water $\delta^{18}O$ associated with the expansion of terrestrial ice sheets since the Middle Miocene must have also affected the isotope records. However, these effects are either too small or in the opposite direction of the observed changes in the $\delta^{18}O$ record (see above).

We calculate the effect of changes in vapor recycling on $\delta^{18}O$ gradients in precipitation as shown in Figure 4a. As described in section 3.1, Nd_{ET} is a metric of vapor recycling as it represents the balance between moisture gain (ET) and moisture lost (Q) (equation (12)). Nd_{ET} will be high for grassland ecosystems where ET approaches P, and thus, Q is low. Conversely, Nd_{ET} will be low for forest ecosystems where $P >$ ET and Q is high. Increasing Nd_{ET} results in a shallower $\delta^{18}O$ gradient (Figure 4a). This results from the fact that when Nd_{ET} is higher, a greater proportion of moisture that falls as precipitation is recycled back to the atmosphere, thereby reducing atmospheric moisture gradients (dw/dx) and increasing characteristic length scales (equation (8)). In other words, with higher Nd_{ET}, the same change in distance along a trajectory results in a smaller decrease in w as shown by the upper axes in Figure 4a [*Winnick et al.*, 2014]. Conversely, the increased input of vapor through ET that is isotopically lighter than the precipitation lost ($\delta_{ET} - \delta_P < 0$)

competes against this effect (equation (6)). The magnitude of this effect in terrestrial systems is less than the effect of increased characteristic lengths and is sensitive to the relative partitioning of E and T (i.e., E/ET and T/ET), as $\delta_E < \delta_T$ due to the equilibrium and kinetic fractionations that occur during E. This competing effect is also reduced in grasslands relative to forests due to the difference in rooting depths and associated $\delta^{18}O$ values of transpiration as discussed above.

Forested regions are characterized by Damköhler numbers ranging from less than 1 to 5 (Figure 2). In contrast, grasslands and arid ecosystems have higher Damköhler numbers (~10 and greater) as the ET flux approaches precipitation in magnitude (Figure 2). Thus, changing hydrologic conditions that allow grasslands to expand will induce a positive isotopic change in $\delta^{18}O$ of precipitation at a given location as depicted by the transition from Point 1 to Point 1′ in Figure 4a. The magnitude of this isotopic change will increase as the distance along the storm track (x') increases.

From this analysis it is evident that the conditions favoring grassland expansion affected the oxygen isotopes of precipitation but is it possible that grasses themselves had substantial effects as well? The influence of grasses on the $\delta^{18}O$ values of precipitation would come from their shallow rooting depths and seasonality of transpiration. It is beyond the scope of this paper to test how seasonality will affect the oxygen isotopes of precipitation (although see *Mix et al.* [2013]). However, we speculate that if grasses were transpiring during their growing season, which is often in the summer months when precipitation is relatively enriched in ^{18}O, then seasonality would tend to increase the $\delta^{18}O$ of precipitation. That said, it is possible to place some quantitative bounds on the effects of rooting depth on the $\delta^{18}O$ values of precipitation using the model presented here.

The oxygen isotope composition of transpired water is generally assumed to be that of precipitation since plants do not fractionate water during uptake [*Dawson and Ehleringer*, 1993]. In environments where $P > E$ this assumption is likely to be true. In this case, transpiration contributes to the isotopic mass balance through the return of nonfractionated water to the atmosphere and the resultant decrease in the horizontal moisture gradient. In semiarid areas where evaporation rates from the soil surface are high, the $\delta^{18}O$ of soil water is greater than the $\delta^{18}O$ of precipitation in the upper half meter of soil [*Hsieh et al.,* 1998; *Ferretti et al.,* 2003] (Figure 3). This effect is the result of the downward diffusion of the heavy isotopologues of water and the upward advection of water toward the evaporating soil surface. In this case, the transpired water will depend upon the rooting depth of the plants. For example, in a study of C3 shrubs and C4 grasses from grassland ecosystems it was found through comparison of the oxygen isotopes of plant xylem and soil water profiles that C4 grasses were sampling the upper 30 cm of the ^{18}O-enriched waters while C3 shrubs were using less fractionated water from deeper in the soil horizon [*Nippert and Knapp*, 2007]. In forest ecosystems, tree roots can extend well pass the soil horizon and, in some cases, have been shown to sample groundwater [*Dawson and Ehleringer*, 1993]. Thus, rooting depth and evaporation of soil water will have an effect on the isotopic composition of transpiration, particularly in grasslands. Here we represent the rooting depths of grasses as the integrated value of $\delta^{18}O$ between 0 and 30 cm and the rooting depth of trees and shrubs as the $\delta^{18}O$ at >1 m [*Jackson et al.,* 1996].

The effects of rooting depth on the $\delta^{18}O$ of precipitation can be as much as vapor recycling alone. For example, under the conditions where the $\delta^{18}O$ of precipitation is sensitive to vapor recycling (Nd_{ET} from 1 to 10), when grasses tap shallow water the change in $\delta^{18}O$ of precipitation nearly doubles the isotopic effect of vapor recycling (Point 1 and Point 1′ in Figure 4b). This observation reflects the fact that grasses will tend to transpire ^{18}O-enriched water in the upper 30 cm of soil, which in turn further reduces the horizontal gradient in $\delta^{18}O$ of atmospheric moisture.

Our analysis also suggests that there is a narrow range of hydrologic conditions over which the $\delta^{18}O$ of precipitation is sensitive to vapor recycling (Figure 5). Today these conditions occur at approximately the transition areas from grasslands and forests, as can be seen in modern gradients in the $\delta^{18}O$ of precipitation [*Liu et al.,* 2010]. The $\delta^{18}O$ of precipitation is sensitive to vapor recycling under conditions that have Damköhler numbers up to about 10, depending upon the E/(ET) ratio (Figure 5). If all of the vapor recycling is a result of evaporation the isotopic effects of vapor recycling will be smaller and occur at lower Damköhler numbers than if all vapor recycling is the result of transpiration (Figure 5). The flattening of the curves is in a sense a "hydrostat," beyond which further recharge of the atmosphere has no effect on the $\delta^{18}O$ of precipitation.

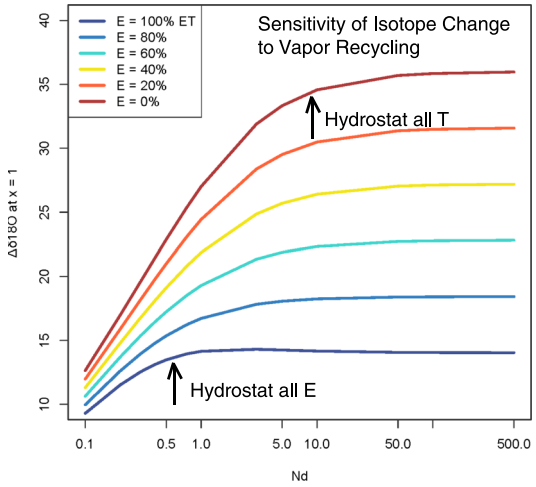

Figure 5. Change in $\delta^{18}O$ at $x' = 1$ relative to the Rayleigh open system case ($Nd_{ET} = 0$) as a function of Nd_{ET} for differing fractions of evaporation and transpiration. Note that these isotopic changes are given for the extreme case where all of the precipitable water is distilled from the air mass (i.e., $x' = 1$).

This result has implications regarding the isotopic records from terrestrial basins (Figure 1). It is not surprising that the positive changes in $\delta^{18}O$ in these basins are diachronous and of varying magnitudes. Since the isotopic effect of vapor recycling occurs at the boundary between forests to grasslands and grasslands to deserts (Figure 2) as the Earth became more arid, any individual isotope profile would record the diachronous spread of this aridity gradient. Moreover, the degree of this positive change in $\delta^{18}O$ would depend upon E/T ratios (Figure 5), which could have varied widely across the globe. Once conditions became sufficiently arid ($Nd_{ET} > 10$, the hydrostat), the isotope profiles become insensitive to degree of vapor recycling. This critical observation may explain the relative stability of some isotope profiles in the arid regions north of Tibet and in North America during the Neogene (Figures S1a–S1e in the supporting information).

Finally, to test whether the reduction of relative humidity during aridification and expansion of grasslands had an effect on the $\delta^{18}O$ of precipitation, we performed a sensitivity analysis of isotopic changes to relative humidity and Damköhler number (Figure 6). Reducing relative humidity steepens the profile in all cases, with the greatest changes occurring at high Damköhler numbers. The primary effect of changing relative humidity in the model is an increase in kinetic fractionation during soil evaporation leading to lower $\delta^{18}O$ values of evaporation, and at high Damköhler numbers this effect is amplified with an increased input of this relatively depleted evaporated water back into the atmosphere. In these simulations, evaporation is set equal to transpiration in order to better examine the model sensitivity to relative humidity; however, this does not accurately represent natural systems. In terrestrial environments, evaporation generally accounts for only 10–20% of evapotranspiration, even in desert (high Damköhler number) ecosystems [*Jasechko et al.,* 2013]. When evaporation is relatively low compared to transpiration, the effect of changing relative humidity becomes insignificant. Thus, our analysis combined with the observation that transpiration dominates the ET fluxes worldwide [*Jasechko et al.,* 2013] suggests that relative humidity played a secondary role in the global changes $\delta^{18}O$ of precipitation (Figure 1).

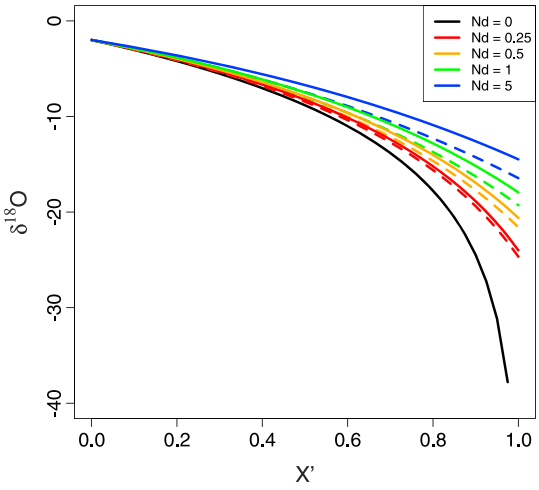

Figure 6. Isotopic profiles in precipitation for different amount of vapor recycling ($Nd_{ET} = 0$ to 5) for relative humidities of 0.5 (dashed lines) to 0.7 (solid lines). For these calculations $E = T$.

5. Implications for Paleoclimate Studies

The fact that changes in plant communities can affect the hydrologic balance has several important implications with regard to paleoclimate and paleoaltimetry reconstructions that rely on stable isotope records. First, in paleoclimate studies where the sites are located in continental interiors with a large fetch the oxygen isotopes of paleoprecipitation proxies will be particularly sensitive to upstream changes in vapor recycling. As an example, when interpreting oxygen isotope records from sites, like the Paleocene-Eocene Thermal Maximum (PETM) in the Bighorn Basin of Wyoming, USA

[*Fricke et al.,* 1998], it is critical to deconvolve the effects of temperature and hydrologic balance induced by plant community changes and aridification. Since we know that there are plant community changes and aridification during this hyperthermal event [e.g., *Wing et al.,* 2005], there should be attendant oxygen isotope changes as a result. The 3 to 4‰ in $\delta^{18}O$ of tooth enamel observed at the PETM that was assigned to temperature increase [*Kraus et al.,* 2013] during the drier PETM could result from conditions in which the Damköhler number increases due to increased vapor recycling relative the runoff. Thus, to understand the isotopic changes in these sites, it is critical to reconstruct time-equivalent horizontal gradients of $\delta^{18}O$ of precipitation from ancient moisture source regions toward continental interiors.

Second, paloealtimetry estimates of past heights of mountain belts will be compromised by vapor recycling in sites within continental interiors, such as Tibet. Because stable isotope paleoaltimetry is based on the fact that ^{18}O- and D-enriched precipitation decreases with elevation, the rise of mountain ranges works in the opposite direction as vapor recycling. The importance of vapor recycling is minimized in studies that examine multiple sites at different elevations on the windward side of mountain ranges [see *Mulch et al.,* 2006]. The minimal importance of vapor recycling results from the fact that equation (10) reduces to Rayleigh distillation as the Damköhler number approaches 0 (i.e., *Q* approaches *P*). However, in continental interiors in which single sites are used to estimate past heights of mountain ranges, like Tibet, the vapor recycling as an air mass moves inward from the moisture source to the mountain range will influence the oxygen isotopic values of precipitation within continental interiors. For example, much of the precipitation reaching the interior of Tibet is sourced from the Indian Ocean and must pass over the Indian subcontinent before it reaches Tibet. Since we know grasslands expanded into this region in the Miocene [*Quade et al.,* 1989a] the isotopic composition of precipitation that reached Tibet after this ecosystem change must have increased in its $\delta^{18}O$ values. Thus, changes in vapor recycling may explain the increase $\delta^{18}O$ values that we observe in paleosols and lake carbonate during the Miocene (see Figures S1a–S1e in the supporting information). In fact, in an elegant study of a site in southwestern Tibet [*Saylor et al.,* 2009] the $\delta^{18}O$ values of Miocene precipitation were found to be lower than modern waters. This difference was interpreted to be the result of a possible lowering of the hypsometric mean elevation of that area since the Miocene. We offer an alternative explanation that the change in $\delta^{18}O$ values of precipitation could be caused by the increased expansion of grasslands within the Indian subcontinent since 9 Ma. This alternative hypothesis is consistent with known plant community changes in this region [*Quade et al.,* 1989a]. That vapor recycling can mask surface uplift is further underscored by recent studies of the Tibetan Plateau that show that vapor recycling has hidden 1.5 to 2 km of surface uplift [*Bershaw et al.,* 2012].

6. Conclusions

We conclude that increased aridity favoring grassland expansion along with grasses themselves conspire to decrease the horizontal gradient of $\delta^{18}O$ values of atmospheric moisture as air masses move into continental interiors. This change in gradient of $\delta^{18}O$ we believe is, in part, responsible for what appears to be a global increase in the $\delta^{18}O$ of precipitation observed on nearly all continents. If correct, these collective isotope records demonstrate the importance of grasslands in modifying the hydrologic budget as they expanded into the midlatitudes during the Miocene.

One critical test of this model would be a comparison of the carbon and oxygen isotope records of continental interiors into which C4 grasses expanded. One would expect that the timing of $\delta^{18}O$ changes of paleosol carbonate should precede that of $\delta^{13}C$ if grasses are affecting gradients in atmospheric vapor downstream of sites they are expanding into. As noted by *Molnar* [2005], this is precisely what is observed in the Indian subcontinent where the $\delta^{18}O$ shift occurs before the change in $\delta^{13}C$. At that time, however, there was no explanation for the diachronous carbon and oxygen isotope records. We suggest that grasses are affecting the $\delta^{18}O$ of precipitation of downstream sites that they have yet expanded into and this would explain the difference in timing of these isotopic records.

Finally, because of the demonstrated importance of vapor recycling by plant communities on the $\delta^{18}O$ of precipitation, it is critical when interpreting stable isotope records from terrestrial settings to assess the role of recycling. To do this, one would reconstruct time-equivalent horizontal gradients of $\delta^{18}O$ of precipitation from moisture source regions toward continental interiors.

Acknowledgments

This research was supported by NSF grants EAR-0609649, EAR-1019648 (CPC), and EAR-0921134 (KM). We thank an anonymous reviewer and Alison Andres for their insightful reviews of this manuscript. We thank Joe Berry and Adam Wolfe for their insightful discussions on biosphere - atmosphere interactions.

References

Allison, G. B. (1982), The relationship between ^{18}O and deuterium in water in sand column undergoing evaporation, *J. Hydrol.*, *55*, 163–169.

Alton, P., R. Fisher, S. Los, and M. Williams (2009), Simulations of global evapotranspiration using semiempirical and mechanistic schemes of plant hydrology, *Global Biogeochem. Cycles*, *23*, GB4023, doi:10.1029/2009GB003540.

Barnes, C. J., and G. B. Allison (1983), The distribution of deuterium and ^{18}O in dry soils 1. Theory, *J. Hydrol.*, *60*, 141–156.

Berry, J., D. J. Beerling, and P. J. Franks (2010), Stomata: Key players in the Earth system, past and present, *Curr. Opin. Plant Biol.*, *13*, 233–240.

Bershaw, J., S. M. Penny, and C. N. Garzione (2012), Stable isotopes of modern water across the Himalaya and eastern Tibetan Plateau: Implications for estimates of paleoelevation and paleoclimate, *J. Geophys. Res.*, *117*, D02110, doi:10.1029/2011JD016132.

Bony, S., C. Risi, and F. Vimeux (2008), Influence of convective processes on the isotopic composition ($\delta^{18}O$ and δD) of precipitation and water vapor in the tropics: 1. Radiative-convective equilibrium and Tropical Ocean-Global-Atmosphere-Coupled-Ocean-Atmosphere Response Experiment (TOGA-COARE) simulations, *J. Geophys. Res.*, *113*, D19305, doi:10.1029/2008JD009942.

Boyce, C. K., and J. E. Lee (2010), An exceptional role for flowering plant physiology in the expansion of tropical forests and biodiversity, *Proc. R. Soc. B*, *277*, 3437–3443, doi:10.1098/rspb.2010.0485.

Breecker, D. O., Z. D. Sharp, and L. D. McFadden (2012), Seasonal bias in the formation of stable isotope composition of pedogenic carbonate in modern soils from central New Mexico, USA, *Geol. Soc. Am. Bull.*, *121*, 630–640.

Cerling, T., Y. Wang, and J. Quade (1993), Expansion of C4 ecosystems as an indicator of global ecological change in the late Miocene, *Nature*, *361*, 344–345.

Dawson, T. E., and J. R. Ehleringer (1993), Isotopic enrichment of water in the "woody" tissues of plants: Implications for plant water source, water uptake, and other studies which use the stable isotopic composition of cellulose, *Geochim. Cosmochim. Ac.*, *57*, 3487–3492.

DePaolo, D. J., M. E. Conrad, K. Maher, and G. W. Gee (2004), Evaporation effects on oxygen and hydrogen isotopes in deep vadose zone pore fluids at Hanford, Washington, *Vadose Zone J.*, *3*, 220–232.

Dettman, D. L., X. Fang, C. N. Garzione, and J. Li (2003), Uplift-driven climate change at 12 Ma: A long $\delta^{18}O$ record from the NE margin of the Tibetan Plateau, *Earth Planet. Sci. Lett.*, *214*, 267–277.

Dugas, W. A., R. A. Hicks, and R. P. Gibbens (1996), Structure and function of C3 and C4 Chihuahuan desert plant communities: Energy balance and components, *J. Arid Environ.*, *34*, 63–79.

Ehleringer, J. R., and T. E. Dawson (1992), Water uptake by plants: Perspectives from stable isotope composition, *Plant, Cell, Environ.*, *15*, 1073–1082.

Evrendilek, F., I. Celik, and S. Kilic (2004), Changes in soil organic carbon and other physical soil properties along adjacent Mediterranean forest, grassland, and cropland ecosystems in Turkey, *J. Arid Environ.*, *59*, 743–752.

Ferretti, D. F., E. Pendall, J. A. Morgan, J. A. Nelson, D. LeCain, and A. R. Mosier (2003), Partitioning evapotranspiration fluxes from a Colorado grassland using stable isotopes: Seasonal variations and ecosystem implications of elevated atmospheric CO_2, *Plant Soil*, *254*, 291–303.

Fricke, H. C., W. C. Clyde, J. R. O'Neil, and P. D. Gingerich (1998), Evidence for rapid climate change in North America during the latest Paleocene thermal maximum: oxygen isotope compositions of biogenic phosphate from the Bighorn Basin (Wyoming), *Earth Planet. Sci. Lett.*, *160*, 193–208.

Garcia-Carreras, L., and D. J. Parker (2011), How does tropical deforestation affect rainfall, *Geophys. Res. Lett.*, *38*, L19802, doi:10.1029/2011GL049099.

Garzione, C. N., P. Molnar, J. C. Libarkin, and B. J. MacFadden (2006), Rapid late Miocene rise of the Bolivian Altiplano: Evidence for removal of mantle lithosphere, *Earth Planet. Sci. Lett.*, *241*, 543–556.

Ghosh, P., J. T. Padia, and R. Mohindra (2004), Stable isotopic studies of paleosol sediment from Upper Siwalik of Himachal Himalaya: Evidence for high monsoonal intensity during late Miocene?, *Palaeogeogr. Palaeoclimatol. Palaeoecol.*, *206*, 103–114.

Gonfiantini, R. (1986), Environmental isotopes in lake studies, in *Handbook of Environmental Isotope Geochemistry*, edited by P. Fritz and J. C. Fontes, pp. 113–168, Elsevier, New York.

Hendricks, M. B. (1999), A one-dimensional model of hydrogen and oxygen isotopic ratios in the global hydrologic cycle, PhD thesis, Chemistry Dept., Univ. of California Berkeley, Berkeley, Calif.

Hendricks, M. B., D. J. DePaolo, and R. C. Cohen (2000), Space and time variation of $\delta^{18}O$ and δD in precipitation: Can paleotemperature be estimated from ice cores?, *Global Biogeochem. Cycles*, *14*, 851–861, doi:10.1029/1999GB001198.

Hetherington, A. M., and F. I. Woodward (2003), The role of stomata in sensing and driving environmental change, *Nature*, *424*, 901–908.

Horita, J., and D. J. Wesolowski (1994), Liquid-vapor fractionation of oxygen and hydrogen isotopes of water from the freezing to the critical temperature, *Geochim. Cosmochim. Acta*, *58*, 3425–3437.

Horton, T. W., and C. P. Chamberlain (2006), Stable isotopic evidence for Neogene surface downdrop in the central Basin and Range Province, *Geol. Soc. Am. Bull.*, *118*, 475–490.

Hsieh, J. C., O. A. Chadwick, E. F. Kelly, and S. M. Savin (1998), Oxygen isotope composition of soil water: Quantifying evaporation and transpiration, *Geoderma*, *82*, 269–294.

Ingraham, N. L., and R. G. Craig (1993), Constraining estimates of evapotranspiration with hydrogen isotopes in a seasonal orographic model, in *Climate Change in Continental Isotopic Record*, *Geophys. Monogr. Ser.*, vol. 78, edited by P. K. Swarte et al., pp. 47–53, AGU, Washington, D. C.

Jackson, R. B., H. A. Mooney, and E. D. Schulze (1996), A global budget for the fine root biomass, surface area, and nutrient contents, *Proc. Natl. Acad. Sci. U.S.A.*, *94*, 7362–7366.

James, S. E., M. Partel, S. D. Wilson, and D. A. Peltzer (2003), Temporal heterogeneity of soil moisture in grassland and forest, *Ecology*, *91*, 234–239.

Janis, C. M. (1993), Mammal evolution in the context of changing climates, vegetation and tectonic events, *Annu. Rev. Ecol. Syst.*, *24*, 467–500.

Jasechko, S., Z. D. Sharp, J. J. Gibson, S. J. Birks, Y. Yi, and P. J. Fawcett (2013), Terrestrial water fluxes dominated by transpiration, *Nature*, *496*, 347–351.

Kanamitsu, M., W. Ebisuzaki, J. Woollen, S.-K. Yang, J. J. Hnilo, M. Fiorino, and G. L. Potter (2002), NCEP-DOE AMIP-II Reanalysis (R-2), *Bull. Am. Meteorol. Soc.*, Nov., 1631–1643.

Kidder, D. L., and E. H. Gierlowski-Kordesch (2005), Impact of grassland radiation on the nonmarine silica cycle and Miocene diatomite, *Palaios*, *20*, 198–206.

Kim, S., and J. R. O'Neil (1997), Equilibrium and nonequilibrium oxygen isotope effects in synthetic carbonates, *Geochim. Cosmochim. Acta*, *61*, 3461–3475.

Kleidon, A., K. Fraedrich, and M. Heimann (2000), A green planet versus a desert world: Estimating the effect of vegetation on the land surface of climate, *Clim. Change*, *44*, 471–493.

Kraus, M. J., F. A. McInerney, S. L. Wing, R. Secord, A. A. Baczynski, and J. I. Bloch (2013), Paleohydrologic response to continental warming during the Paleocene-Eocene Thermal Maximum, Bighorn Basin, Wyoming, *Paleaogeogr. Palaeoclimatol. Palaeoecol.*, *370*, 196–208.

Kurc, S. A., and E. E. Small (2004), Dynamics of evapotranspiration in semiarid grassland and shrubland ecosystems during the summer monsoon season, central New Mexico, *Water Resour. Res.*, *40*, W09305, doi:10.1029/2004WR003068.
Lee, J. E., and I. Fung (2007), "Amount effect" of water isotopes and quantitative analysis of post-condensation processes, *Hydrol. Process.*, *22*, 1–8, doi:10.1002/hyp.6637.
Lee, J. E., et al. (2012), Reduction of tropical land region precipitation variability via transpiration, *Geophys. Res. Lett.*, *39*, L19704, doi:10.1029/2012GL053417.
Liu, B., F. M. Phillips, and A. R. Campbell (1996), Stable carbon and oxygen isotopes of pedogenic carbonates, Ajo Mountains, southern Arizona: Implications for paleoenvironmental change, *Paleaogeogr. Palaeoclimatol. Palaeoecol*, *124*, 233–246.
Liu, Z., G. J. Bowen, and J. M. Welker (2010), Atmospheric circulation is reflected in precipitation isotope gradients over the conterminous United States, *J. Geophys. Res.*, *115*, D22120, doi:10.1029/2010JD014175.
Mix, H. T., M. J. Winnick, A. Mulch, and C. P. Chamberlain (2013), Grassland expansion as an instrument of hydrologic change in Neogene western North America, *Earth Planet. Sci. Lett.*, *377–378*, 73–83.
Molnar, P. (2005), Mio-Pliocene growth of the Tibetan Plateau and evolution of east Asian climate, *Palaeontologia Electronica*, *8*, 2–23.
Mulch, A., S. A. Graham, and C. P. Chamberlain (2006), Hydrogen isotopes in Eocene river gravels and paleoelevation of the Sierra Nevada, *Science*, *313*, 87–89.
Nippert, J. B., and A. K. Knapp (2007), Linking water uptake with rooting patterns in grassland species, *Oecologia*, doi:10.1007/s00442-007-0745-8.
Oki, T., and S. Kanae (2006), Global hydrological cycles and world water sources, *Science*, *313*, 1068–1072.
Osborne, C. P. (2008), Atmosphere, ecology and evolution: What drove the Miocene expansion of C_4 grasslands?, *Ecology*, *96*, 35–45.
Poulsen, C. J., and M. L. Jeffery (2011), Climate change imprinting on stable isotopic compositions of high-elevation meteoric water cloaks past surface elevations of major orogens, *Geology*, *39*, 595–598.
Quade, J., T. E. Cerling, and J. R. Bowman (1989a), Development of Asian monsoon revealed by marked ecological shift during the latest Miocene in northern Pakistan, *Nature*, *342*, 163–166.
Quade, J., T. E. Cerling, and J. R. Bowman (1989b), Systematic variations in the carbon and oxygen isotopic composition of pedogenic carbonate along elevational transects in the southern Great Basin, United States, *Geol. Soc. Am. Bull.*, *101*, 464–475.
Quade, J., N. Solounias, and T. E. Cerling (1994), Stable isotopic evidence from paleosol carbonates and fossil teeth for forest or woodlands in Greece over the past 11 Ma, *Paleaogeogr. Palaeoclimatol. Palaeoecol.*, *108*, 41–53.
Retallack, G. J. (2001), Cenozoic expansion of grasslands and climatic cooling, *J. Geol.*, *109*, 407–426.
Risi, C., S. Bony, and F. Vimeux (2008), Influence of convective processes on the isotopic composition ($\delta^{18}O$ and δD) of precipitation and water vapor in the tropics: 2. Physical interpretation of the amount effect, *J. Geophys. Res.*, *113*, D19306, doi:10.1029/2008JD009943.
Rozanski, K., L. Aragufis-Aragufisa, and R. Gonfiantini (1993), Isotopic patterns in modern global precipitation, in *Climate Change in Continental Isotopic Record*, *Geophys. Monogr. Ser.*, vol. 78, edited by P. K. Swarte et al., pp. 1–36, AGU, Washington, D. C.
Running, S. W., and J. C. Coughlan (1988), A general model of forest ecosystem processes for regional applications: Hydrologic balance, canopy gas exchange and primary production processes, *Ecol. Modell.*, *42*, 125–154.
Saylor, J. E., J. Quade, D. L. Dettman, P. G. DeCelles, P. A. Kapp, and L. Ding (2009), The Late Miocene through present paleoelevation history of southwestern Tibet, *Am. J. Sci.*, *309*, 1–42.
Takeuchi, A., and P. B. Larson (2005), Oxygen isotope evidence for the late Cenozoic development of an orographic rain shadow in eastern Washington, *Geology*, *223*, 127–146.
Wilson, K. B., P. J. Hanson, P. J. Mulholland, D. D. Baldocchi, and S. D. Wullschleger (2001), A comparison of methods for determining evapotranspiration and its components: Sap-flow, soil water budget, eddy covariance and catchment water balance, *Agric. For. Meteorol.*, *106*, 153–168.
Wilson, M., and J. Paz-Ferreiro (2012), Effects of soil-use intensity on selected properties of mollisols in Entre Rios, Argentina, *Comm. Soil Sci. Plant Anal.*, *43*, 71–80.
Wing, S. L., G. J. Harrington, F. A. Smith, J. I. Bloch, D. M. Boyer, and K. H. Freeman (2005), Transient floral change and rapid global warming at the Paleocene–Eocene boundary, *Science*, *310*, 993–996.
Winnick, M. J., C. P. Chamberlain, J. K. Caves, J. M. Welker (2014) Quantifying the isotopic "continental effect", *Earth Planet. Sci. Lett.*, doi:10.1016/j.epsl.2014.09.005.
Zachos, J., M. Pagani, L. Sloan, E. Thomas, and K. Billups (2001), Trends, rhythms, and aberrations in global climate 65 Ma to Present, *Science*, *292*, 686–693.
Zimmermann, U., D. Ehhalt, and K. O. Munnich (1967), Soil-water movement and evapotranspiration: Changes in the isotopic composition of water, in *Isotopes and Hydrology*, pp. 567–586, International Atomic Energy Agency, Vienna, Austria.